

Summary

Introduction

Rapid environmental change, IPCC, estimated temperature rise.

Trend to precocity in plants, flowering time, etc. Advance in phenology.

Problem: Understanding (and predicting?) long-lived plant adaptation to climate change

Based on previously developed demographic and quantitative genetics model (see), added fluctuating environments. Made theoretical predictions. Estimated fluctuations using data from phenological data (PHENOFIT).

Materials and Methods

Population model

We used a previously developed model with stage-structure (Sandell 2014, master's thesis). We considered a population of trees split in two classes, immature (I) and mature (M). only mature individuals reproduce. Each year, an immature individual can survive with a probability s_I , mature and reproduce with a probability of m . At the same time, a mature individual has a probability s_M to survive. First-time reproducers, i.e. immature that became mature and reproduce the same year, have a fecundity of f_1 , while experienced reproducers, those who already reproduced at least once, have a fecundity of f_2 . Produced seeds have a probability s_0 to survive and join the pool of immature trees. The standard parameters set is given in (Table 1). The population census is just before reproduction. The population dynamics can be predicted using the following matrix (Caswell, 2001):

$$A = \begin{pmatrix} a_{II} & a_{IM} \\ a_{MI} & a_{MM} \end{pmatrix} = \begin{pmatrix} s_0 m f_1 + s_I(1 - m) & s_0 f_2 \\ s_M m & s_M \end{pmatrix} \quad (1)$$

, where a_{ij} , the transition rate, describes the contribution of stage j individuals to stage i the next year. With given initial conditions we can compute the number of individuals in the two stages by iterating matrix multiplication by A .

I implemented density-dependence in this model, so that the population would not continuously increase (see Figure 1). I assumed seed germination and survival parameter s_0 declined with increasing density of mature and immature competitors using a Beverton-Holt function (Caswell, 2001):

$$s_0 = \frac{s_{0,max}}{1 + k_I N_I + k_M N_M} \quad (2)$$

with k_I and k_M the weights of immature (N_I) and mature (N_M) population respectively. $s_{0,max}$ is the maximum achievable s_0 .

Phenotype and life-history traits

We model the evolution of a phenotypic trait, e.g. the date at which first leafs appear on a tree, z the bud-burst date. In our model, an individual is born with a given phenotype and keeps it throughout its life.

Too early bud-burst can compromise the survival of young immature trees and the fecundity of mature trees because of the risk of frost. Too late bud-burst also affects the same traits because the bad season arrives before enough photosynthetates have been accumulated to guarantee survival of young trees and maturation of fruits. We assume that the survival of large mature trees is less sensitive to

variation of phenology. We therefore supposed that for each individual - s_I immature survival, f_1 first reproducers fecundity and f_2 experienced reproducers - (see Equation 1) to be Gaussian function of phenotype z . Thus, bud-burst date directly influence their values. They are expressed as follow:

$$\begin{cases} s_I(z) = s_I(\theta_s) \exp\left(-\frac{(z - \theta_s)^2}{2\omega_s}\right) \\ f_1(z) = f_1(\theta_f) \exp\left(-\frac{(z - \theta_f)^2}{2\omega_f}\right) \\ f_2(z) = f_2(\theta_f) \exp\left(-\frac{(z - \theta_f)^2}{2\omega_f}\right) \end{cases} \quad (3)$$

, θ_s is the optimal bud-burst date for survival, i.e. phenotype where s_I is at its maximum $s_I(\theta_s)$; ω_s is the width of the Gaussian function, its inversely related to selection intensity: with small ω_s values, only a restricted range of bud-burst dates would have important survival rates. f_1 and f_2 have similar expressions, but the optimal bud-burst date θ_f is different from θ_s , f_1 and f_2 only differ by their maximum values $f_i(\theta_f)$, with f_1 lower than f_2 (see Table 1 to have standard parameters values).

The optimal trait values θ_s and θ_f can differ between stages and life-history components, but trait value does not change along the life of an individual, then there is a trade-off between the two fitness components fecundity and immature survival. The evolution of the trait then affects the population dynamics through the life-history of the individuals in the population.

If we want to compute mean transition rate $\overline{a_{ij}}$, we need to average s_I , f_1 and f_2 (ex: $\overline{a_{IM}} = s_0 \overline{f_2}$):

$$E[s_I] = \overline{s_I} = \int p_I(z) s_I(z) dz \quad (4)$$

, with $p_I(z)$ the distribution of z in the immature stage. We suppose p_I has a Gaussian distribution with mean $\overline{z_I}$ and width P_I the phenotypic variance in the immature stage (Lande, 1982). We end with the following expression for $\overline{s_I}$:

$$\overline{s_I}(\overline{z_I}) = s_I(\theta_s) \sqrt{\frac{\omega_s}{\omega_s + P_I}} \exp\left(-\frac{(\overline{z_I} - \theta_s)^2}{2(\omega_s + P_I)}\right) \quad (5)$$

We obtain similar expressions for $\overline{f_1}$ and $\overline{f_2}$.

Iterations at each time step

Assuming the phenotype has a Gaussian distribution, the mean genotypic value of matures and immatures at the next time step is given by (Barfield et al. 2011 Eq.5, applied to the current models)

:

$$\overline{g_I}' = (c_{IM}\overline{g_M} + c_{II}\overline{g_I}) + (c_{IM}G_M\beta_{a_{IM}} + c_{II}G_I\beta_{a_{II}}) \quad (6a)$$

$$\overline{g_M}' = (c_{MI}\overline{g_I} + c_{MM}\overline{g_M}) + (c_{MI}G_I\beta_{a_{MI}} + c_{MM}G_M\beta_{a_{MM}}) \quad (6b)$$

with $c_{ij} = \frac{n_j \overline{a_{ij}}}{n'_i}$, the contribution of stage j individuals to next years pool of stage i individuals, as a fraction of i individuals at the next time step n'_i ; and $\beta_{a_{ij}}$ the selection gradient as $\beta_{a_{ij}} = \frac{\partial \ln \overline{a_{ij}}}{\partial \overline{z}}$ (Barfield et al., 2011). The selection gradient represents the force of directional selection, and together with the genetic variance for the trait (G), is used to predict the change in mean phenotype due to the response to selection (Lande, 1982).

The first term is a weighted average of mean genotypes contributing to this stage; while the second shows the effect of selection.

To have the formal expressions of $\beta_{a_{ij}}$ we need to compute the selection gradients on life-history components:

$$\begin{aligned}\beta_{\bar{s}_I} &= \frac{\partial \ln \bar{s}_I}{\partial \bar{z}_I} = \frac{\theta_s - \bar{z}_I}{\omega_s + P_I} \\ \beta_{\bar{f}_1} &= \frac{\partial \ln \bar{f}_1}{\partial \bar{z}_I} = \frac{\theta_f - \bar{z}_I}{\omega_f + P_I} \\ \beta_{\bar{f}_2} &= \frac{\partial \ln \bar{f}_2}{\partial \bar{z}_M} = \frac{\theta_f - \bar{z}_M}{\omega_f + P_M}\end{aligned}\quad (7)$$

Because we have for example $\bar{a}_{II} = s_0 m \bar{f}_1 + \bar{s}_I (1 - m)$ we get the selection gradient:

$$\beta_{a_{II}} = \frac{s_0 m \bar{f}_1 \beta_{\bar{f}_1} + \bar{s}_I \beta_{\bar{s}_I} (1 - m)}{\bar{a}_{II}} \quad (8)$$

We have a similar recursion for phenotypes (Barfield et al., 2011). We need to distinguish direct transitions of individuals from one stage to the other \bar{t}_{ij} and events leading to new individuals \bar{f}_{ij} (note $\bar{a}_{ij} = \bar{t}_{ij} + \bar{f}_{ij}$), because in the first case the phenotype remain unchanged while in the second only the genotype is inherited:

$$\bar{z}'_I = c_{II}^t(\bar{z}_I + P_I \beta_{t_{II}}) + c_{II}^f(\bar{g}_I + G_I \beta_{f_{II}}) + c_{IM}^f(\bar{g}_M + G_M \beta_{f_{IM}}) \quad (9a)$$

$$\bar{z}'_M = c_{MI}^t(\bar{z}_I + P_I + \beta_{t_{MI}}) + c_{MM}^t(\bar{z}_M + P_M + \beta_{t_{MM}}) \quad (9b)$$

, with $\beta_{t_{ij}}$ the gradient of selection defined as above in Equation 6a, i.e. $\beta_{t_{ij}} = \frac{\partial \ln \bar{t}_{ij}}{\partial \bar{z}}$; $c_{ij}^t = \frac{n_j \bar{t}_{ij}}{n'_i}$ the contribution by direct transition of stage j to stage i and $c_{ij}^f = \frac{n_j \bar{f}_{ij}}{n'_i}$ the contribution by birth.

Approximation under weak selection

Under weak selection, the mean phenotype at equilibrium in the population \bar{z} follows in a constant environment (Engen et al., 2011):

$$\bar{z}_{eq} = \frac{\gamma_f \theta_f + \gamma_s \theta_s}{\gamma_f + \gamma_s} \quad (10)$$

, with,

$$\gamma_f = \frac{v_I u_I s_0 m \bar{f}_1}{\lambda(P_I + \omega_f)} + \frac{v_I u_M \frac{G_M}{G_I} s_0 \bar{f}_2}{\lambda(P_M + \omega_f)} \quad (11a)$$

and

$$\gamma_s = \frac{v_I u_I \bar{s}_I (1 - m)}{\lambda(P_I + \omega_s)} \quad (11b)$$

γ_f and γ_s represent the respective weight of each of the optimum in the trade-off between θ_f and θ_s for \bar{z}_{eq} . Indeed, if $\theta_f = \theta_s$ then $\bar{z}_{eq} = \theta_f = \theta_s$. But if $\theta_f \neq \theta_s$, then the position of the mean phenotype depends on γ_f and γ_s .

Fluctuating optimums

I introduced environmental fluctuations in the model through the optima:

$$\begin{cases} \theta_f(t) = \bar{\theta}_f + \alpha_f \xi_f \\ \theta_s(t) = \bar{\theta}_s + \alpha_s \xi_s \end{cases} \quad (12)$$

α_i is the sensitivity of θ_i to noise ξ_i . ξ_f and ξ_s are noise vectors drawn at each time step from a bi-variate normal distribution with respectively σ_f^2 and σ_s^2 variances and correlation ρ_N .

Under varying environment we get another approximation under weak selection from (Engen et al., 2011) describing the change of mean phenotype:

$$\Delta \bar{z}(t) = -G_I \gamma (\bar{z}(t) - \theta_v(t)) \quad (13)$$

, with

$$\gamma = \gamma_f + \gamma_s \quad (14a)$$

$$\theta_v(t) = \bar{z}_{eq} + \xi_v \quad (14b)$$

$$\xi_v = \frac{\alpha_f \xi_f + \alpha_s \xi_s}{\alpha_f + \alpha_s} \quad (14c)$$

We see that the change in the mean phenotype depends on the sensitivity of the optima α_i as well as on the magnitude of the variations.

Trend in change

To model climate-change, and especially the trend of increasing temperature with time, we included a trend in the variation of the optima:

$$\begin{cases} \theta_i(t) = \bar{\theta}_i + \alpha_i \epsilon(t) \\ \epsilon(t) = kt + \xi_i \end{cases} \quad (15)$$

With k having a negative value, the optima tend to decrease with time.

PHENOFIT data

PHENOFIT is a phenology model including several sub-models, from environmental and phenological data it simulates the survival and reproduction of an average tree to predict its range (Morin et al., 2008).

We used output from PHENOFIT (simulations performed by A. Duputié) from 1950 to 2100 for the sessile oak (*Quercus petraea*) about predicted bud burst date and predicted fitnesses in 6 localities (see Figure 4). We had fitness and fecundity predictions for phenotypes around the modeled date (a range of 21 days). From these data we predicted the optima fluctuations. Considering fecundity f as a Gaussian function around this date with the same form as f_1 in Equation 5:

$$\beta = \frac{\partial \ln f}{\partial \bar{z}} = \frac{\theta_f - \bar{z}}{\omega_f + \sigma_z^2} \quad (16)$$

Using (Lande and Arnold, 1983), with z Gaussian, $p(z)$ the distribution of z in the population, $f(z)$ the fitness associated with z and \bar{f} the mean fitness in the population, we computed selection gradients from PHENOFIT simulation outputs as:

$$\beta = \frac{\text{cov}(z, \frac{f(z)}{\bar{z}})}{\sigma_z^2} \quad (17)$$

From (16) and (17) we can express θ_f :

$$\theta_f = \frac{\text{cov}(z, \frac{f(z)}{\bar{z}})}{\sigma_z^2} (\omega_f + \sigma_z^2) + \bar{z} \quad (18)$$

In our estimations we considered $p(z)$ to be Gaussian around the modeled date by PHENOFIT, with a variance of $P_I = 40$ as in our analytic model. We normalized this distribution so that all dates in the population would be in the 42 days interval around the modeled date.

Trend analyses

All statistical analyses were made using R (R Core Team, 2014), graphics were drawn using ggplot2 (Wickham, 2009), data were handled using dplyr (Wickham and Francois, 2014).

To estimate the trend of the θ_f variations, we considered a trend model with three components: a general decreasing linear trend, a white noise component with a constant variance and a more dramatic noise leading to "catastrophic" events, with low θ_f values.

The regular noise and the trend were estimated excluding those catastrophic events, we kept only value of θ_f over 60, which is the lower bound of the realizable range of bud burst date of oak trees. Then we performed a linear regression between values of θ_f and time, giving us an estimation of k from Equation 15. Analyzing the residuals gives us the variance of $\alpha_f \xi_f$ from the same equation.

Results

Constant environment and density-dependence

We used the previously developed model in (Sandell 2014) and simulated (see Figure 1) a tree population for 150 years in a constant environment, with and without density-dependence on s_0 , assess the effects of a more realistic demography.

As expected, density-dependence allows regulating the population (Figure 1 right panel), as the number of mature and immature individuals seem to converge respectively to 18000 and 10000 individuals, while without density-dependence the population is exponentially growing.

Looking at the phenotype, we started from exactly the same starting point $z = 116$ for phenotypic and genotypic values. Without density-dependence, the population quickly converge to the equilibrium phenotype ($\overline{z_{weak}}$ given by the approximation in Equation 10), $\overline{z_{eq}} = 116$ in this case. With density-dependence the equilibrium phenotype is shifted towards the survival optimum θ_s ($\overline{z_{weak,dd}} = 121.8$, $\theta_s = 130$ while $\theta_f = 100$). The lower seed survival s_0 decreases γ_f (11a) changing the weights in (10), making it more interesting to favor the survival of already established immature trees than the production of many propagules with very little survival prospect.

The genotypic values, $\overline{g_I}$ and $\overline{g_M}$ (respectively gray and black on Figure 1) are clearly distinct from the mean phenotype values.

The mean immature phenotype $\overline{z_I}$ converge quicker than the mean mature phenotype $\overline{z_M}$ to $\overline{z_{eq}}$. High mature trees survival in our simulations makes it long to replace them with a different genotype and phenotype. To make $\overline{z_M}$ closer to $\overline{z_{eq}}$, immature individuals with a phenotype closer to $\overline{z_{eq}}$ need to survive long enough to mature and outnumber initial mature individuals with phenotype further from $\overline{z_{eq}}$.

Fluctuating optima

To mimic a changing environment we made the optima fluctuate (Figure 2, dashed lines) and compared this model to the one in constant environment (solid lines).

The mean phenotype of the population does not change very much with the fluctuations, indeed, $\overline{z_M}$ in constant and fluctuating environment are equal, and they are also equal to $\overline{z_{eq}}$, that is why they are indistinguishable on Figure 2.

Only $\overline{z_I}$ fluctuates under varying environment, but the fluctuations have a very small variance compared to the ones of the optima. We found a strong correlation between θ_s and $\overline{z_I}$ across years

($\rho_{\text{Pearson}} = 0.6997364$) than with θ_f . It shows how immature individuals track the variations of the survival optimum and invest specifically more on this fitness component.

Because of the variations the phenotype lags away from the optimal value, decreasing the mean of s_I in fluctuating environment. The number of immature individuals N_I is thus lower under the fluctuating regime then decreasing the number of mature individuals N_M , this decline in density in turn increases s_0 . The variation in θ_s causes s_I to decrease, it reveals the cost of the fluctuations demographically: fluctuating regime causes variations in survival that may have dramatic effect on population.

However, those fluctuations do not seem to affect fecundities f_1 and f_2 in the same way (Figure 2 bottom left panel). As the mean optima move they get closer to population phenotype increasing fecundity, but the next time step they move further away from this phenotype and they decrease fecundity.

The asymmetry of responses between survival s_I and fecundities f_1 and f_2 , are explained by the specific trade-off occurring in our population. The mean phenotype in our simulations is closer to θ_s than to θ_f , there is a higher chance of θ_s to be lower or much higher than the mean population phenotype, then there is for θ_f to cross the mean population phenotype line.

As we had partially correlated noises in our population (see Table 1 to have standard parameters set), we vary correlations for noises between 0 and 1. The results were similar whatever the correlation coefficient. It seemed that the lower the correlation between noises, the higher were the demographic burden (results unshown). Uncorrelated environments decrease more the life-history traits than correlated environments.

Trend in the environment

We implemented a decreasing trend in θ_f with fluctuations (Figure 3) to mimic climate change. We simulated both a linear trend and a linear trend with fluctuations in optima variation (respectively solid and dashed lines in Figure 3).

The phenotype in the population decreases as the optima decrease, but much slower, whether with fluctuations or not. The mean phenotype in the immature stage \bar{z}_I seem to vary in the same fashion with and without fluctuations, while the mean phenotypes among mature individuals \bar{z}_M are almost indistinguishable in the two types of environments, \bar{z}_M under fluctuations (dashed line) is a little bit over \bar{z}_M without them (solid line). We implemented the approximation \bar{z}_e from (Engen et al., 2011), it seems to follow the variations in a similar fashion as the mean phenotype of the mature individuals.

The immature survival (s_I) has an interesting behavior, it first increases, reaches a maximum, then decreases. The decreasing trend in optima variation causes at first the mean population phenotype to move closer to θ_s , thus maximizing s_I values when it crosses θ_s line, as soon as it moves beyond s_I starts to decrease again.

On the contrary f_1 and f_2 the mean population phenotype go further away from θ_f with and without fluctuation.

After a certain number of years, population is lower in environments with trends than in constant ones, the effect is especially visible in the environments without fluctuations (Figure 2 & Figure 3 bottom right panel). However, fluctuations in constant environment seem to decrease more the number of immature individuals than the trend does in constant environment.

As expected, the decreasing trend in θ_f creates a lag between the optima and the mean population values, because adaptation is slower than the rate of change. However, the population can still survive with such a rate if the difference between the optima and the means become constant. On a very long scale (2500 years) it is what happens in this case, the population maintains itself by changing its phenotype fast enough to track the optima variation (data not shown).

Estimation of the fluctuations

In 6 localities (map [Figure 4](#) bottom left) using PHENOFIT output, we computed θ_f values at these locations (top 3 rows of [Figure 4](#)). For the 6 sites, predicted θ_f decreases with time: earlier bud-burst is favored as climate warms.

Over the general trend, we observe a small amplitude variation, corresponding to year to year change in θ_f and some more episodic dramatic decreases in its values, sometimes reaching negative values (e.g. at BIC site in 1976). The frequency of these events increase with time as they become common after 2050 for all sites. Note that those events are biased towards the decrease of θ_f , as there is no equivalent dramatic increases.

The negative values of θ_f computed in [Figure 4](#), may seem striking as there is no such thing as a negative bud-burst date! It indicates strong directional selection to shorten bud-burst those years with very little sign of quadratic selection on that trait. As bottom right panel of [Figure 4](#) shows, we can have negative value of θ_f and still have achievable phenotypes. If θ_f is very negative for a given year (less than -100 in 2048 for LAB), it means there will be no reproduction this year (flat tail of blue curve, bottom right panel [Figure 4](#)).

We excluded those extreme events, taking all sites together, to estimate the trend in the variation of θ_f (see [Materials and Methods](#)). Using linear regression on θ_f with time, we found a rate of $-0.15\text{day}\cdot\text{year}^{-1}$, with normal residuals having a variance of 105day^2 (data not shown, $R^2 = 0.2341$, $p < 2\text{e-}16$, $F = 186.7$ with 611 d.f.).

Discussion

We modeled a stage-structured tree population using a quantitative genetics approach, with bud-burst date the studied trait varying between two optima. We used it to understand their phenotype evolution in the next 150 years. Using PHENOFIT simulation results we computed values for one of the optima. An increasing number of extreme events would happen in the next century.

As expected in the literature, we found a decreasing trend in the variation of optima, i.e. a trend to precocity of phenology ([Aitken et al., 2008](#); [Ehrlén and Münzbergová, 2009](#)). Because of the general increase in temperature, organisms advance their phenology to track their original environment.

Long-lived stage structure populations don't have show strong reaction to fluctuations nor to climate change -> beware of the "buffer" effect, due to life cycle

Fluctuations don't have strong effect on phenotype but on demography

Increasing number of catastrophic events

Our model -> need more realistic variations including "catastrophic events", include phenotypic plasticity, understand better the difference between breeding values and phenotypes, predict extinction time?

References

- Aitken, S. N., Yeaman, S., Holliday, J. A., Wang, T. and Curtis-McLane, S. (2008). Adaptation, migration or extirpation: climate change outcomes for tree populations. *Evolutionary Applications* 1, 95--111.
- Barfield, M., Holt, R. D. and Gomulkiewicz, R. (2011). Evolution in Stage-Structured Populations (2 versions). *The American Naturalist* 177, 397--409.
- Caswell, H. (2001). Matrix population models : construction, analysis, and interpretation. Sinauer Associates.

- Ehrlén, J. and Münzbergová, Z. (2009). Timing of Flowering: Opposed Selection on Different Fitness Components and Trait Covariation. *The American Naturalist* 173, 819--830.
- Engen, S., Lande, R. and Sæther, B.-E. (2011). Evolution of a Plastic Quantitative Trait in an Age-Structured Population in a Fluctuating Environment. *Evolution* 65, 2893--2906.
- Lande, R. (1982). A Quantitative Genetic Theory of Life History Evolution. *Ecology* 63, 607--615.
- Lande, R. and Arnold, S. J. (1983). The Measurement of Selection on Correlated Characters. *Evolution* 37, 1210--1226.
- Morin, X., Viner, D. and Chuine, I. (2008). Tree species range shifts at a continental scale: new predictive insights from a process-based model. *Journal of Ecology* 96, 784--794.
- R Core Team (2014). R: A Language and Environment for Statistical Computing. R Foundation for Statistical Computing Vienna, Austria.
- Wickham, H. (2009). *ggplot2: elegant graphics for data analysis*. Springer New York.
- Wickham, H. and Francois, R. (2014). *dplyr: A Grammar of Data Manipulation*. R package version 0.3.0.2.

| Parameter | Notation | Value |
|---|---|-------|
| Life Cycle | | |
| Optimal phenotype for fecundity | θ_f | 100 |
| Optimal phenotype for immature survival | θ_s | 130 |
| Fecundity function width | ω_f | 400 |
| Survival function width | ω_s | 400 |
| Heritability | h^2 | 0.5 |
| Phenotypic variance of immatures | P_I | 40 |
| Phenotypic variance of matures | P_M | 40 |
| Genotypic variance of immatures | $G_I = P_I \times h^2$ | 20 |
| Genotypic variance of matures | G_M | 20 |
| Survival of immature at phenotypic optimum | $\overline{s_I}(\overline{z} = \theta_s)$ | 0.8 |
| Fecundity of first time reproducers at optimum | $\overline{f_1}(\overline{z} = \theta_f)$ | 100 |
| Fecundity of experienced reproducers at optimum | $\overline{f_2}(\overline{z} = \theta_f)$ | 200 |
| Maturation rate of immature | m | 0.02 |
| Combined survival and germination rate of seed | s_0 | 0.03 |
| Survival of mature stage | s_M | 0.99 |
| Density-dependence | | |
| Maximum s_0 in density-dependence function | $s_{0,max}$ | 0.12 |
| Decreasing factor due to immatures | k_I | 0.001 |
| Decreasing factor due to matures | k_M | 0.005 |
| Fluctuations | | |
| Sensitivity of optimum for fecundity to fluctuation | α_f | 5 |
| Sensitivity of optimum for survival to fluctuation | α_s | 5 |
| Noise variance for fecundity | $\sigma_{\xi_f}^2$ | 3.725 |
| Noise variance for survival | $\sigma_{\xi_s}^2$ | 3.725 |
| Correlation between noises | ρ_N | 0.5 |
| Trend coefficient | k | -0.15 |

Table 1: Standard parameter set

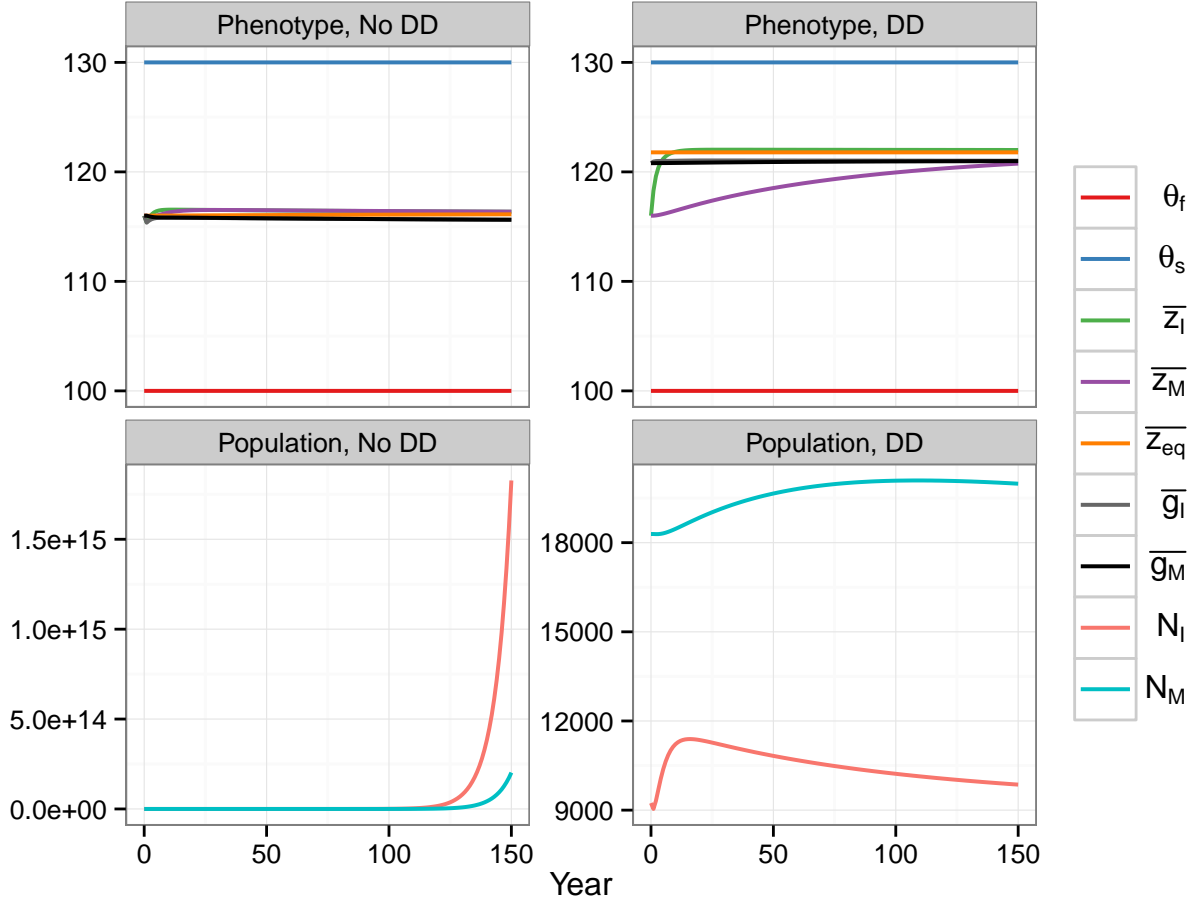


Figure 1: Effect of density-dependence on phenotypes and populations. **Top:** Phenotype variations in population (\bar{z}_I, \bar{z}_M , starting from $z = 116$) with their corresponding genotypic values (\bar{g}_I, \bar{g}_M), and the approximation given by Equation 10; **Bottom:** Population, number of immature individuals (N_I , red), number of mature individuals (N_M , blue). Starting from Stable-Stage Distribution (SSD) in constant environment. **No DD** means we used the model without density-dependence, **DD** means we implemented density-dependence through s_0 (see Equation 2). Here, bud-burst date is expressed in julian days (numbered days in the year, 1st of January being 1 in julian days).

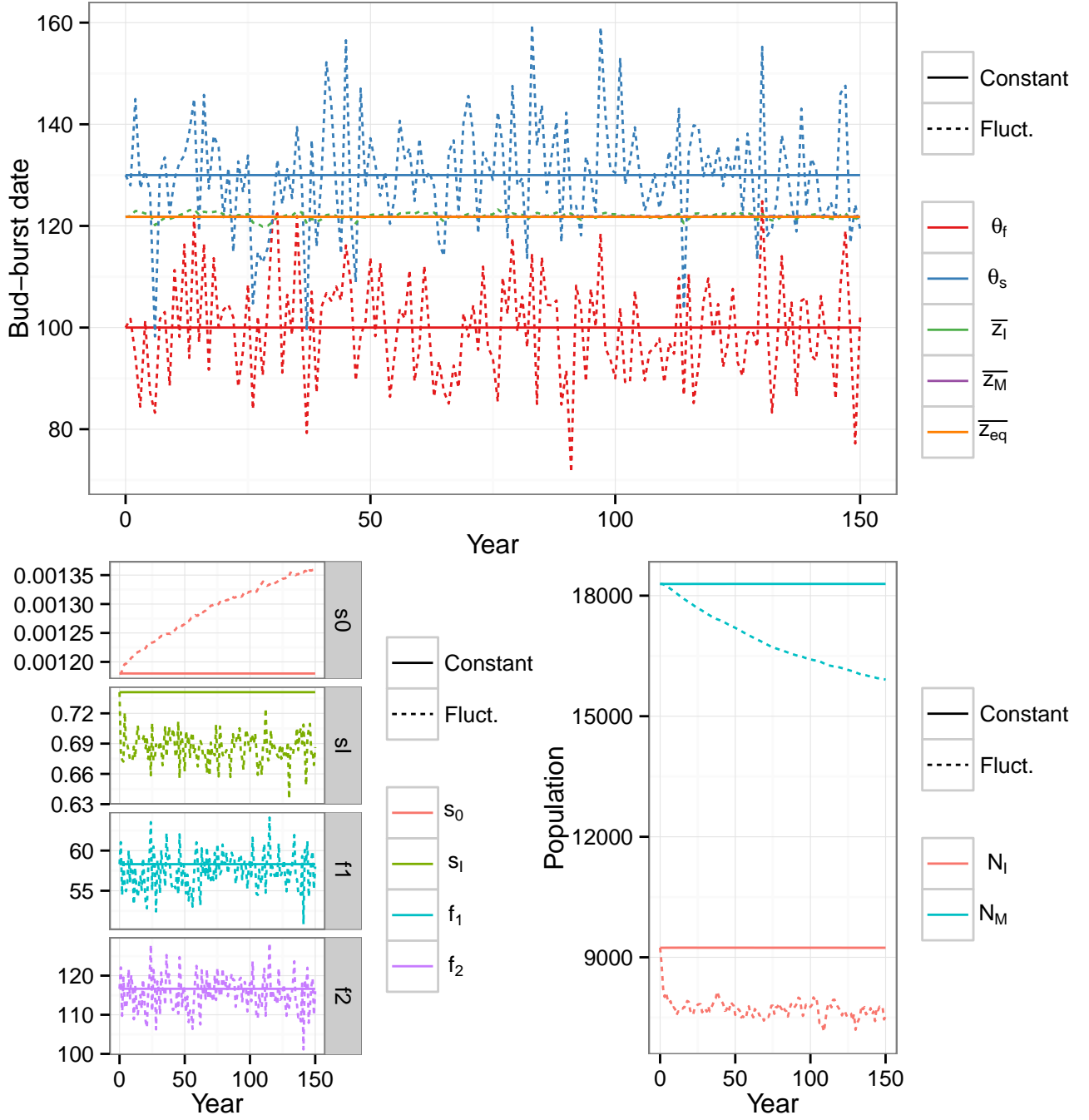


Figure 2: Fluctuating optima against constant environment. **Top:** comparison of phenotypes from simulations with constant or fluctuating optima, \bar{z}_{eq} is the approximation shown in Equation 10 results from single simulation. **Bottom: (Left)** life-history traits in constant or fluctuating environment, **(Right)** population in constant or fluctuating environment, N_I is the number of immature individuals and N_M the number of mature individuals, population started from the stable stage distribution. **Solid lines:** values in constant environment, **Dashed lines:** in fluctuating environment, results were averaged over 100 independent simulations.

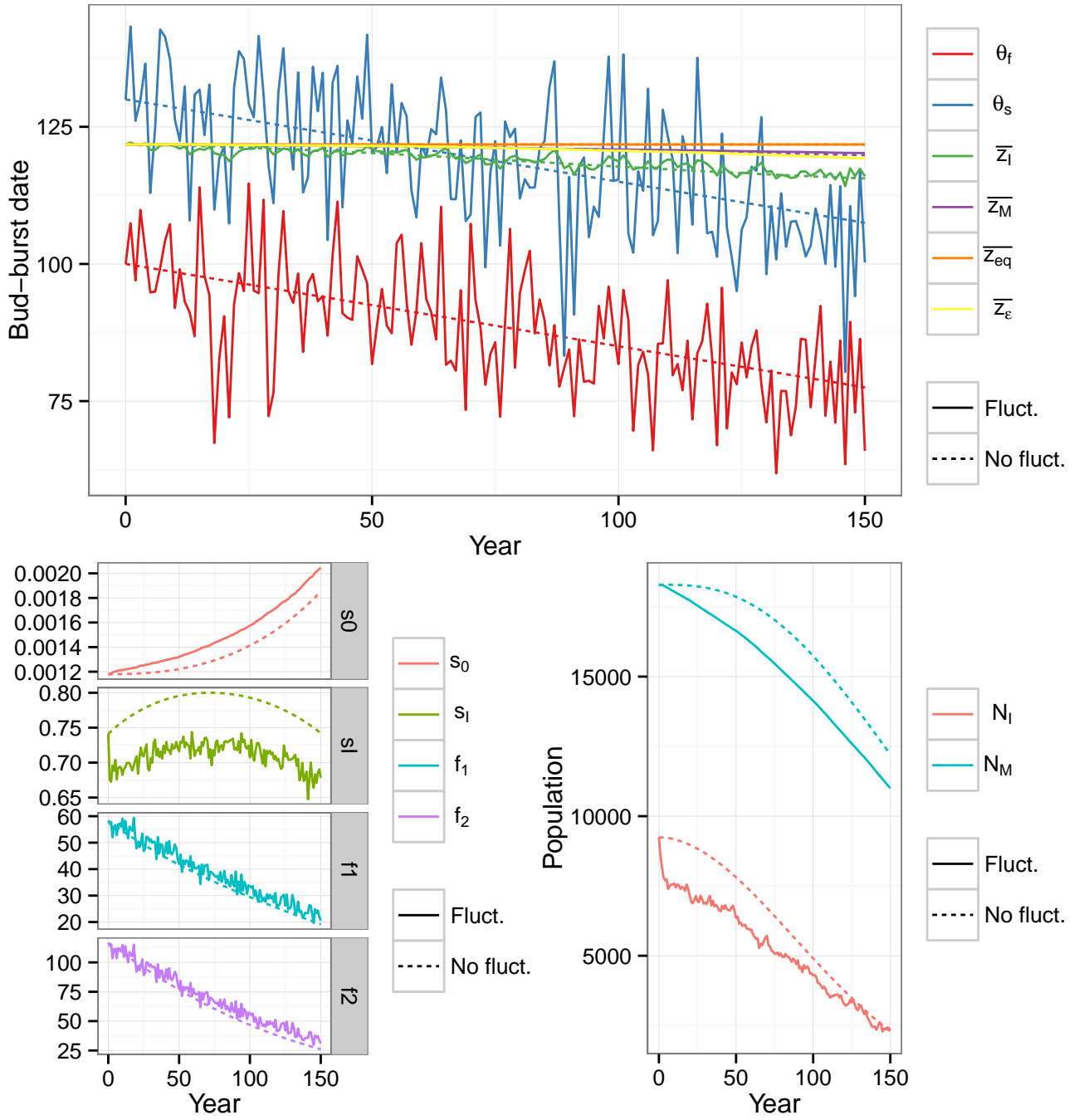


Figure 3: Mixed influences of trend and fluctuations on the population. **Top:** Phenotype evolution with and without fluctuations, results from a **single** simulation; **Bottom: (Left)** life-history traits evolution; **(Right)** demography. **Solid lines: (No fluct.)** linearly decreasing optima with time; **Dashed lines: With fluct.** fluctuating decreasing optima, results were averaged over 100 independent simulations.

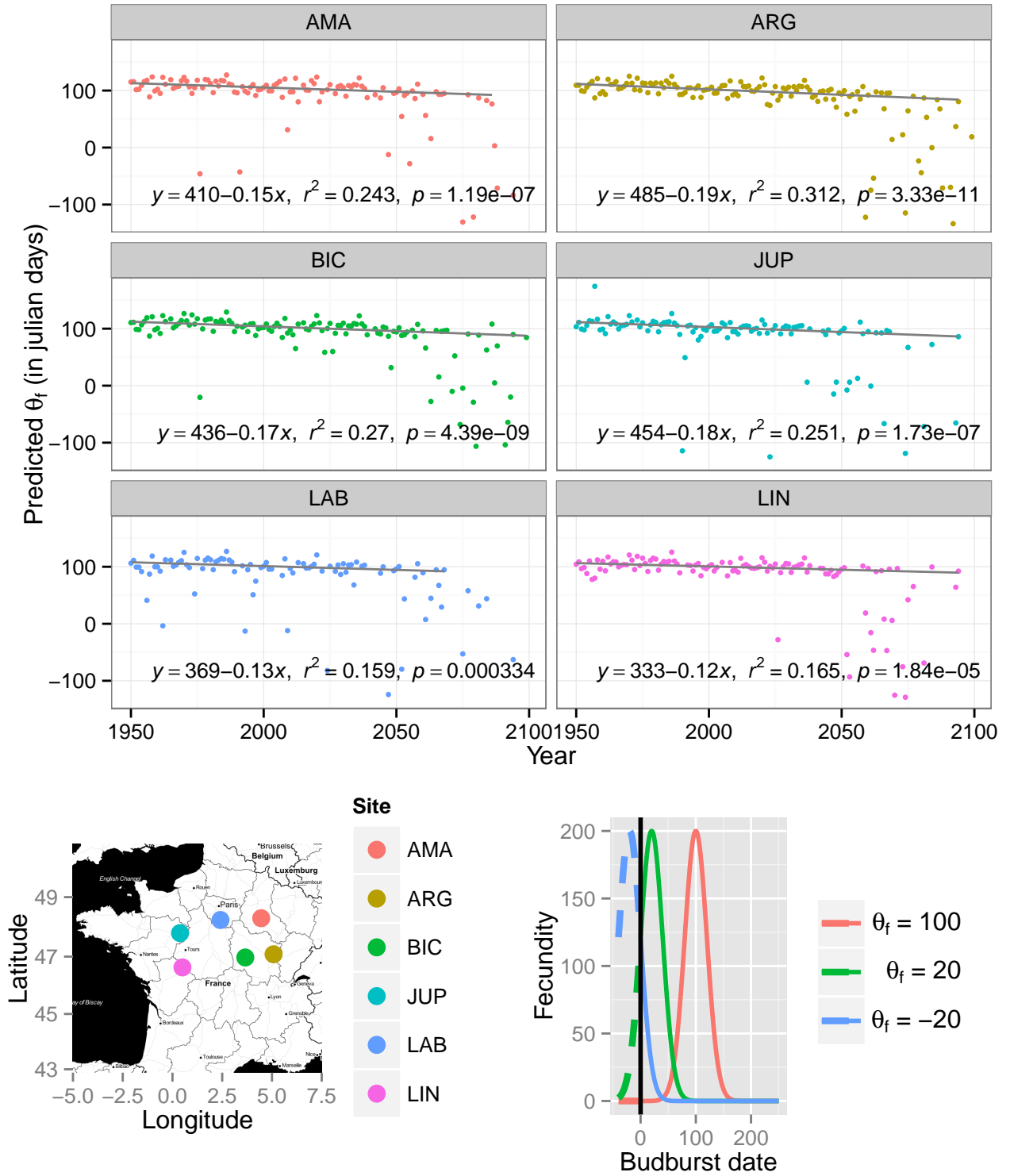


Figure 4: θ_f estimations from PHENOFIT data. **Top:** estimations of θ_f for each study site (see [Materials and Methods](#) for details). **Bottom: (Left)** map of the study sites; **(Right)** Theoretical fecundity functions with parameters from [Table 1](#) with values of θ_f equals to 100, 20 and -20, solid lines indicate achievable phenotype, dashed lines show theoretical curves but unreachable phenotypes.